JOURNAL OF QUATERNARY SCIENCE (2011) 26(1) 37–43 ISSN 0267-8179. DOI: 10.1002/jqs.1424

Glacier fluctuations in the southern Peruvian Andes during the late-glacial period, constrained with cosmogenic ^{3}He

GORDON R.M. BROMLEY,[1]* BRENDA L. HALL,[1] JOERG M. SCHAEFER,[2] GISELA WINCKLER,[2] CLAIRE E. TODD[3] and KURT M. RADEMAKER[1]

[1]Department of Earth Sciences/Climate Change Institute, Edward T. Bryand Global Science Center, University of Maine, Orono, Maine 04469-5790, USA

[2]Lamont-Doherty Earth Observatory/Department of Earth and Environmental Sciences of Columbia University, Comer Geochemistry, Palisades, New York, USA

[3]Department of Geological Sciences, Rieke Science Center, Pacific Lutheran University, Tacoma, Washington, USA

Received 5 January 2010; Revised 18 May 2010; Accepted 26 May 2010

ABSTRACT: The occurrence of pronounced climate reversals during the last glacial termination has long been recognised in palaeoclimate records from both hemispheres and from high to low latitudes. Accurate constraint of both the timing and magnitude of events, such as the Younger Dryas and Antarctic Cold Reversal, is vital in order to test different hypotheses for the causes and propagation of abrupt climate change. However, in contrast to higher-latitude regions, well-dated records from the Tropics are rare and the structure of late-glacial tropical climate remains uncertain. As a step toward addressing this problem, we present an *in situ* cosmogenic ^{3}He surface exposure chronology from Nevado Coropuna, southern Peru, documenting a significant fluctuation of the ice margin during the late-glacial period. Ten tightly clustered ages from a pair of moraines located halfway between the modern glacier and the Last Glacial Maximum terminus range from 11.9 to 13.9 ka and give an arithmetic mean age of 12.8 ± 0.7 ka (1σ). These data constitute direct evidence for a readvance, or prolonged stillstand, of glaciers in the arid Andes of southwestern Peru. Copyright © 2011 John Wiley & Sons, Ltd.

KEYWORDS: late-glacial reversal; last termination; Tropics; cosmogenic helium-3; glaciers.

Introduction

The last glacial–interglacial transition ('Termination 1') represents the most significant reorganisation of Earth's climate in the last 100 ka. Imposed upon the pattern of rising global temperatures, distinct and sometimes abrupt climate oscillations have been recognised in numerous proxy records from sites worldwide. In the classic view of the late-glacial period, events in the Northern Hemisphere typically are tied to the Younger Dryas (YD: 11.6–12.9 ka), an abrupt return to near full-glacial conditions first identified in Scandinavia (Blytt, 1876; Sernander, 1908; Mangerud *et al.*, 1974). In a similar sense, several recent investigations in the Southern Hemisphere (Fogwill and Kubik, 2005; Moreno *et al.*, 2009) have correlated late-glacial events with the slightly earlier Antarctic Cold Reversal (ACR: 12.9–14.5 ka). The importance of understanding abrupt, suborbital climate change (Denton *et al.*, 2005) has prompted a substantial body of research directed towards constraining the geographic extent of events such as the YD (e.g. Denton and Hendy, 1994; Gosse *et al.*, 1995; Briner *et al.*, 2002; Ackert *et al.*, 2008). In the Tropics, for example, a YD signature has been recognised in precipitation records (Schulz *et al.*, 1998; Hughen *et al.*, 2000; Haug *et al.*, 2001; Wang *et al.*, 2001), suggesting that cold events in the North Atlantic region are intricately linked to changes in the distribution of low-latitude rainfall.

Resolving the exact timing, structure and geographic extent of late-glacial climate events is fundamental to our understanding of the causes of abrupt climate change and poses a key problem in palaeoclimate research (Denton *et al.*, 2005). Nonetheless, the response of glaciers to late-glacial climate variability remains an unresolved and controversial issue. Glaciers are sensitive indicators of climate change (Oerlemans, 2001; Anderson and Mackintosh, 2006), advancing and retreating in response to small changes in temperature and precipitation, and have the potential to provide valuable, long-term records of climate. Our understanding of past glacier behaviour at tropical latitudes is limited, however, by low spatial resolution of data and insufficient dating resolution (Rodbell *et al.*, 2009).

The occurrence of a late-glacial climate reversal in the tropical Andes of South America has been debated for decades (Mercer and Palacios, 1977; Clapperton and McEwan, 1985; Schubert and Clapperton, 1990; Hansen, 1995; Clapperton *et al.*, 1997; Rodbell and Seltzer, 2000) and continues to be contentious. In their comprehensive review of Andean glacier records, Rodbell *et al.* (2009) noted that most tropical moraines of late-glacial age are constrained either by minimum- or maximum-bounding radiocarbon ages, and that few are dated sufficiently to identify discrete patterns in climate behaviour. Adding to the uncertainty, tropical moraine chronologies based on surface exposure dating – an increasingly common practice in the Andes – are subject to significant systematic uncertainties at these latitudes and altitudes due to ambiguity in nuclide production rates and scaling schemes (Farber *et al.*, 2005; Zech *et al.*, 2007, 2008; Smith *et al.*, 2008; Bromley *et al.*, 2009), requiring a conservative approach to interpreting cosmogenic ages.

In their recent review of published data, Rodbell *et al.* (2009) suggested that a YD-like signal occurs in various records from the tropical Andes, a view supported by at least two recent studies (Mahaney *et al.*, 2007; Glasser *et al.*, 2009). Nonetheless, compelling evidence for this event remains elusive (Smith *et al.*, 2008) and indications of an advance during the ACR in southeastern Peru (Goodman *et al.*, 2001) and, potentially, in northern Bolivia (Blard *et al.*, 2009) emphasise that the pattern of late-glacial climate behaviour in the tropical Andes is far from resolved (Rodbell *et al.*, 2009). This uncertainty represents a significant shortcoming of our knowledge both of millennial and submillennial climatic variability in the Tropics, and of the global extent of abrupt climate change events.

As an important step toward addressing this problem, we present 10 cosmogenic ^{3}He surface exposure ages from late-

*Correspondence: G. R. M. Bromley, as above.
E-mail: gordon.bromley@umit.maine.edu

glacial moraines on Nevado Coropuna in southwestern Peru. The moraines are located midway between the modern glacier terminus and moraines dated to the Last Glacial Maximum (LGM; Bromley *et al.*, 2009). We calculated these ages using currently accepted scaling protocols (Balco *et al.*, 2008) and a compilation of global ^{3}He production rates (Goehring *et al.*, 2010).

Geological and climatic overview

Nevado Coropuna (6426 m; 15° 33′ S, 72° 93′ W), located 150 km northwest of Arequipa (Fig. 1), is both the highest peak in the Cordillera Ampato and the highest volcano in Peru. The mountain comprises four andesite domes separated by broad saddles and rises ~2000 m above the surrounding puna on all but the south side. Here, incision of the underlying ignimbrite by the Rio Llacllaja, a tributary of the Colca Canyon, has resulted in relief of more than 3500 m. Although andesitic eruptions at Coropuna began during the late Miocene, the mountain's present structure is attributed to prolonged Quaternary volcanism (Venturelli *et al.*, 1978; Weibel *et al.*, 1978). The most recent activity produced three large andesite flows on the west, north and south flanks (Fig. 2). Although these flows have not been dated directly, they overlie deposits of known late-glacial age (Bromley *et al.*, 2009; this study) and, in turn, have been eroded by subsequent glacial activity.

The persistent inversion over the Pacific coast and strong Andean rain shadow effect combine to maintain a semi-arid climate at Coropuna. Most precipitation (~390 mm water equivalent a^{-1} at 6080 m; Herreros *et al.*, 2009) arrives during the brief summer wet season (December–March). Coropuna currently supports an ice cap (~60 km^2; Racoviteanu *et al.*, 2007) drained by 15 outlet glaciers, as well as extensive perennial snow. Due to aridity, glaciers are restricted to elevations significantly higher (5100–5500 m) than the local zero-degree isotherm (~4900 m; Dornbusch, 1998) and ablation occurs both by melting and sublimation. Today, meltwater streams are rare and flow only during clear conditions. The largest drains the ice cap via the north-flowing valley of Quebrada Ullullo (Fig. 2). Glaciofluvial features associated with Late Pleistocene moraines indicate the presence of former melting margins.

Glacial–geological overview

Abundant, well-preserved glacial deposits on the slopes of Coropuna correspond to periods when ice was more extensive than today. Dornbusch (2002) described moraines on the mountain's west flank as corresponding to a single, undated event. This record was expanded by Bromley *et al.* (2009) to include evidence both for older and younger events registered in several locations on Coropuna. In addition, Bromley *et al.* (2009) presented a preliminary cosmogenic ^{3}He surface exposure moraine chronology and demonstrated the suitability of the ^{3}He method for use in the tropical Andes. The most striking glacial landforms on Coropuna include large lateral moraines, some as much as 100 m in relief and 8 km long (Fig. 3), radiating out from the mountain. Bromley *et al.* (2009) attributed these moraines (C-I) to the LGM, between ca. 21 and 25 ka. Beyond the LGM limit, moraines and drift corresponding to at least two earlier advances are preserved on the plateau north and east of Coropuna (Fig. 3).

On all sides of Coropuna, a prominent set of bouldery moraines (C-II) occurs midway between the LGM termini and the modern ice margin and corresponds to a readvance, or prolonged stillstand, of glaciers during deglaciation (Bromley *et al.*, 2009). The best-preserved C-II deposits are located in the north-facing Quebrada Santiago (Figs 2 and 3) and are the focus of this study. Bromley *et al.* (2009) provided four preliminary cosmogenic ^{3}He ages from this complex and suggested it was deposited during the late-glacial period.

Figure 1. Map of Peru showing locations of Nevado Coropuna (NC) and the Cordillera Blanca (CB).

Sampling and analysis methods

The geomorphic mapping of C-II moraines in Quebrada Santiago forms the basis of this study and is described in detail by Bromley *et al.* (2009). To obtain a ^{3}He surface exposure chronology, we sampled the tops of andesite boulders (0.5–3 m high) located on lateral- and end-moraine crests (Fig. 4). We collected the upper few centimetres (≤5 cm) of rock beneath boulder surfaces. Boulder surfaces typically exhibit glacial polish and striae, indicating that post-depositional granular erosion and spallation have been negligible. The size of the samples and the arid conditions at Coropuna minimise shielding effects due to snow or vegetation. We acknowledge the possibility of post-depositional exhumation of boulders, due to erosion or deflation of moraines, but suggest that this process has been minimal on Coropuna due to aridity and the bouldery, sharp-crested nature of the C-II moraines.

We measured helium concentrations in small (125–250 μm diameter) clinopyroxene (augite) minerals. Rock samples were first crushed and sieved to retrieve the 125–250 μm size fraction. Using heavy liquids, magnetic separation and hand-picking, we then separated the pyroxenes. Gases from the pyroxene separates were released by total extraction at ~1300–1400°C for 15 min, during which time the furnace was kept exposed to a liquid nitrogen-cooled charcoal trap for gas purification. We purified the gases further by exposing them to an SAES getter at room temperature. Residual gas was collected on a cryogenically cooled trap held at ~13 K and helium then was separated from neon by heating the trap to 45 K. Abundance and isotopic analyses were performed with an MAP 215-50 noble gas mass spectrometer calibrated with a known volume of a Yellowstone helium standard (MM) with a ^{3}He/^{4}He ratio of 16.45R_a, where $R_a = (^3\text{He}/^4\text{He})_{\underline{air}} = 1.384 \times 10^{-6}$. Mass spectrometry measurements were conducted at Lamont-Doherty Earth Observatory following the protocol of Winckler *et al.* (2005). ^{3}He/^{4}He ratios of the investigated rocks are extremely high, ranging from 9 to 19 times the atmospheric ratio (Table 2). Therefore, we do not correct our dataset for non-cosmogenic (e.g. magmatic) ^{3}He as such corrections would be less than 1%.

We present the ^{3}He ages calculated using globally derived production rates for ^{3}He (Goehring *et al.*, 2010) and the Lm

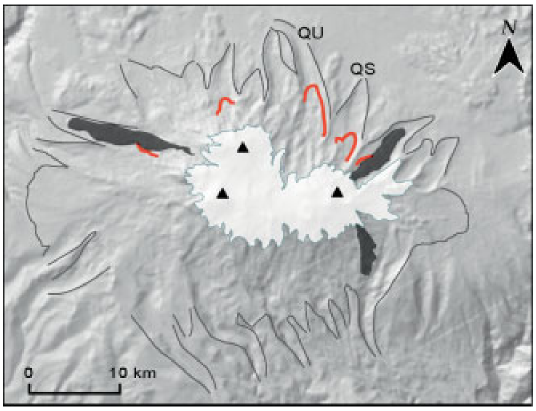

Figure 2. Map of Coropuna showing Quebradas Santiago (QS) and Ullullo (QU), postglacial lava flows (black) and glacial limits: black lines, LGM moraines; red lines late glacial moraines.

Figure 4. Sampling boulder (NC34) on C-II moraine crest, Quebrada Santiago.

(Lal, 1991/Stone, 2000/Nishiizumi *et al.*, 1989) and Li (Lifton *et al.*, 2005) scaling models (Balco *et al.*, 2008, as modified by Goehring *et al.*, 2010: see Bromley *et al.*, 2009, for a detailed description of our calculation methodology). Our interpretations and discussion are based on the results of the time-dependent Lm scaling, because it is used widely and incorporates geomagnetic variability at low latitudes. Furthermore, ^{10}Be production rate calibration studies from both Peru (Farber *et al.*, 2005) and New Zealand (Putnam *et al.*, 2010) have shown that at test sites the Lm scaling gives the closest match to available radiocarbon constraints (N. Lifton, pers. comm., 2009). We also include here four ages reported by us previously (NC17–20: Bromley *et al.*, 2009), now recalculated to be consistent with out new data.

Results

C-II deposits preserved in Quebrada Santiago form a closely spaced pair of right-lateral moraines descending to a pair of terminal moraines at ~5000 m. The paired moraines merge to form a single left-lateral moraine (Figs 3 and 5). The length (~1.25 km in *Q.* Santiago, 2.9 km in *Q.* Ullullo), large size, and continuous nature of the lateral moraines suggest that these deposits represent an advance of ice, as opposed to a pause in recession. Moreover, the steep distal slopes of C-II moraines are indicative of deposition along a robust, steep ice margin, a configuration typical of advancing glaciers. By contrast, recessional landforms on Coropuna typically form short, low-relief sections of end moraines with gentle distal slopes and little or no continuity up-valley. Nonetheless, although the morphology of the C-II moraines is strongly indicative of deposition at the margins of advancing glaciers, we acknowledge the possibility that the moraines instead represent a prolonged stillstand during post-LGM deglaciation.

The C-II moraines are prominent, bouldery ridges of 5–10 m relief that exhibit well-defined crests 1–5 m in width. An exception occurs where the left-lateral moraine crosses a bedrock escarpment, becoming instead a thin, bouldery drift unit with a well-defined edge (Figs 3 and 5). This drift edge extends upslope for ~350 m before merging with the continuation of the left-lateral moraine Figs 3 and 5). Moraines with similar morphology, relative position and weathering occur in neighbouring valleys (Fig. 2) and elsewhere on the mountain (Bromley *et al.*, 2009).

Altogether, there are 12 cosmogenic ^{3}He ages from the C-II deposits in Quebrada Santiago. Four samples (NC17–20: Bromley *et al.*, 2009) were from the prominent drift edge, described above. We collected an additional six samples from the moraine complex itself: one (NC33) from the outer end moraine, four (NC32, 34–36) from the inner end moraine, one (NC37) from the left-lateral moraine below the drift edge and two (NC38, 39) from the left-lateral moraine upslope of the drift edge (Fig. 5). Sample and helium data are given in Tables 1 and 2 and surface exposure ages in Table 3. Together, ^{3}He surface exposure ages from the C-II moraines range from 11.9 ± 0.5 to 13.9 ± 0.3 ka (Fig. 5; Table 3), with an arithmetic

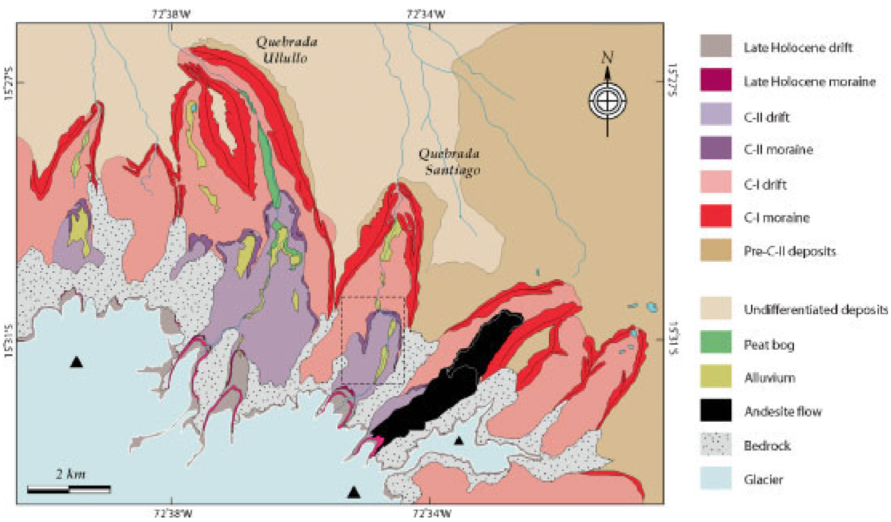

Figure 3. Geomorphic map of Quebrada Santiago area. Dashed line indicates the area shown in Fig. 5.

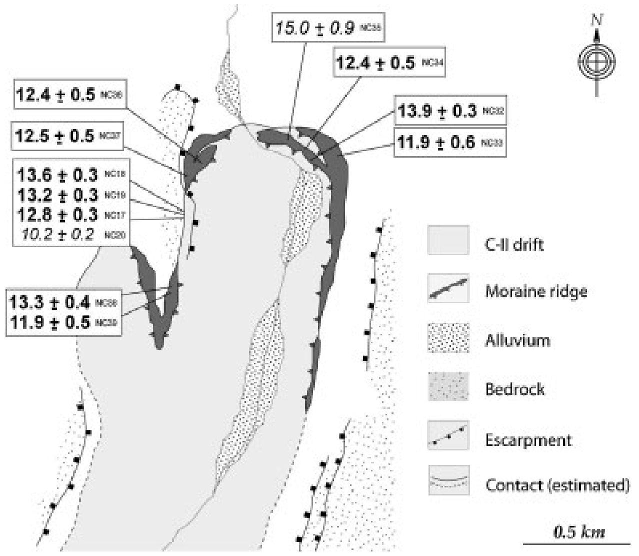

Figure 5. Close-up map of Quebrada Santiago showing distribution of C-II moraines and ^{3}He ages.

mean age of 12.8 ± 0.7 ka (1σ). Plotted as a probability curve, the C-II ages exhibit a slightly bimodal distribution (Fig. 6), with a principal peak age of 13.4 ka and a secondary peak age of 12.4 ka. We exclude samples NC20 and 35 as young and old outliers, respectively, both being more than 2σ beyond the mean.

Discussion

The moraine record from Quebrada Santiago indicates that post-LGM retreat was interrupted by a glacier advance or stillstand, during which the C-II moraines were deposited. At this time, the glacier terminus was located approximately mid-distance between the modern ice edge and the LGM limit (Fig. 7), suggesting that a significant portion of deglaciation already had taken place. The dearth of retreat moraines or downwasting deposits up-valley of the C-II limits, both in Quebrada Santiago and in other valleys on Coropuna, indicates that subsequent recession largely was inactive or was too rapid for moraine formation. Thus the C-II deposits represent a unique event between the LGM and the presumed late Holocene moraines.

Regardless of scaling scheme, the 10 ages from C-II moraines in Quebrada Santiago exhibit a high degree of internal consistency. With Lm scaling, these data constrain the event unequivocally to the late-glacial period. With Li scaling the age range becomes significantly younger at 9.5–10.9 ka and would suggest an early Holocene age for the advance. We consider this unlikely, however, given both substantial evidence for full interglacial conditions in the tropical Andes by the early Holocene (e.g. Thompson *et al.*, 1995, 1998; Seltzer *et al.*, 2002; Ramirez *et al.*, 2003; Bush *et al.*, 2005) and the absence of known events in the early Holocene that might have caused glaciers to advance to half their LGM extent. Therefore, we reiterate that we base our interpretations on the Lm dataset.

Table 1. Sample data and helium concentrations for C-II moraines.

Sample no.	Lat. S	Long. W	Altitude (m)	Type	Thickness (cm)	Shielding	$^3He_{cos}$ (atoms g^{-1})	1σ
NC17*	−15.511	−72.5860	5082	Cobble	6.3	0.967	1.862×10^7	4.351×10^5
NC18*	−15.5112	−72.5862	5087	Cobble	7	0.997	1.977×10^7	4.229×10^5
NC19*	−15.5114	−72.5862	5087	Cobble	6	0.983	1.924×10^7	5.464×10^5
NC20*	−15.5116	−72.5861	5089	Cobble	6	0.997	1.493×10^7	3.589×10^5
NC32	−15.5089	−72.5799	5034	Boulder	3	0.997	2.031×10^7	4.92×10^5
NC33	−15.511	−72.5782	5063	Boulder	5	0.993	1.767×10^7	9.619×10^5
NC34	−15.5102	−72.5786	5052	Boulder	1.5	0.995	1.85×10^7	7.368×10^5
NC35	−15.0994	−72.5786	5052	Boulder	1.6	0.995	2.254×10^7	1.293×10^6
NC36	−15.5096	−72.5855	5053	Boulder	3.25	0.998	1.818×10^7	6.873×10^5
NC37	−15.5105	−72.5861	5066	Boulder	3.1	0.982	1.821×10^7	6.886×10^5
NC38	−15.5115	−72.5862	5095	Boulder	5	0.997	1.939×10^7	6.597×10^5
NC39	−15.5139	−72.5869	5130	Boulder	2	0.998	1.832×10^7	8.336×10^5

Density (all samples) = 2.7 g cm^{-3}; erosion (all samples) = 0 mm a^{-1}. *Samples of Bromley *et al.* (2009), recalculated here according to Balco *et al.* (2008), with the modification of Goehring *et al.* (2010).

Table 2. Helium isotope data for all C-II samples. ^{3}He/^{4}He ratios are given as measured and relative to the atmospheric ^{3}He/^{4}He value.

Sample no.	^{3}He/^{4}He	^{3}He/^{4}He (R/R_a)	1σ	^{4}He (atoms g^{-1})	1σ	^{3}He (atoms g^{-1})	1σ
NC17*	1.571×10^{-5}	11	4.729×10^{-7}	1.185×10^{12}	2.232×10^{10}	1.862×10^7	4.351×10^5
NC18*	1.738×10^{-5}	13	4.782×10^{-7}	1.138×10^{12}	1.952×10^{10}	1.977×10^7	4.229×10^5
NC19*	1.845×10^{-5}	13	6.204×10^{-7}	1.043×10^{12}	1.864×10^{10}	1.924×10^7	5.464×10^5
NC20*	1.343×10^{-5}	10	3.978×10^{-7}	1.112×10^{12}	1.911×10^{10}	1.493×10^7	3.589×10^5
NC32	1.538×10^{-5}	11	3.415×10^{-7}	1.433×10^{11}	1.387×10^9	2.031×10^7	4.92×10^5
NC33	1.243×10^{-5}	9	6.595×10^{-7}	1.434×10^{11}	1.749×10^9	1.767×10^7	9.619×10^5
NC34	2.234×10^{-5}	16	8.372×10^{-7}	9.04×10^{10}	1.22×10^9	1.85×10^7	7.368×10^5
NC35	2.611×10^{-5}	19	1.428×10^{-6}	8.855×10^{10}	1.542×10^9	2.254×10^7	1.293×10^6
NC36	1.856×10^{-5}	13	6.777×10^{-7}	1.371×10^{11}	1.344×10^9	1.818×10^7	6.873×10^5
NC37	2.004×10^{-5}	14	6.905×10^{-7}	1.044×10^{11}	1.628×10^9	1.821×10^7	6.886×10^5
NC38	1.98×10^{-5}	14	6.08×10^{-7}	9.765×10^{10}	1.428×10^9	1.939×10^7	6.597×10^5
NC39	2.353×10^{-5}	17	1.017×10^{-6}	8.29×10^{10}	1.18×10^9	1.832×10^7	8.336×10^5

$R_a = 1.384 \times 10^{-6}$. *See Table 1 footnote.

Table 3. C-II surface exposure ages calculated according to the Lm (time-dependent) and Li scaling schemes of Balco *et al.* (2008).

Sample no.	Lm (ka)	Li (ka)
Production rate (atoms g^{-1} a^{-1})	120 ± 9.4	136 ± 4.1
NC17*	12.8 ± 0.3	10.2 ± 0.2
NC18*	13.6 ± 0.3	10.9 ± 0.2
NC19*	13.2 ± 0.4	10.5 ± 0.3
NC20*	10.2 ± 0.2†	8.0 ± 0.2†
NC32	13.9 ± 0.3	11.1 ± 0.3
NC33	11.9 ± 0.7	9.5 ± 0.5
NC34	12.4 ± 0.5	9.9 ± 0.4
NC35	15.0 ± 0.9†	12.2 ± 0.7†
NC36	12.4 ± 0.5	9.9 ± 0.4
NC37	12.5 ± 0.5	10.0 ± 0.4
NC38	13.3 ± 0.5	10.6 ± 0.4
NC39	11.9 ± 05	9.5 ± 0.4
Age range	11.9 – 13.9	9.5 – 11.1
Mean age	12.8 ± 0.7	10.2 ± 0.5

* See Table 1 footnote. † Daggers denote outliers.

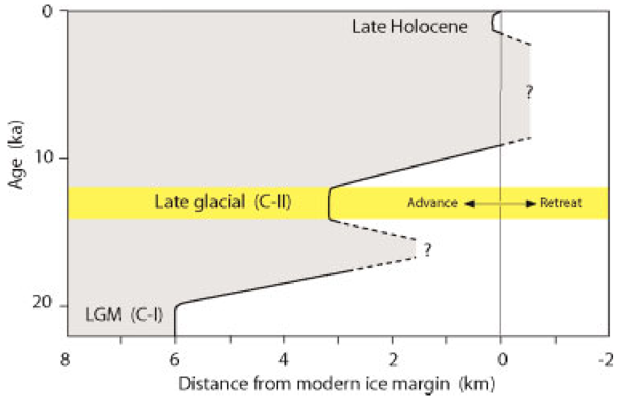

Figure 7. Age–distance diagram depicting former ice front positions in Quebrada Santiago relative to today. Constraint of the LGM (C-I) event is based on ages from Bromley *et al.* (2009). The late-glacial (C-II) advance is constrained by ages given in this study. Although no ages exist for late Holocene moraines, for the purpose of this diagram we assign them a 19th-century age, consistent with the last major advance documented elsewhere in the Peruvian Andes (Kaser, 1999; Solomina *et al.*, 2007; Licciardi *et al.*, 2009). Dashed lines indicate inferred glacier extent.

The C-II ages range from 11.9 to 13.9 ka and exhibit two peaks of similar size at 12.7 and 13.4 ka (Fig. 6). It is possible that this bimodal distribution represents two distinct age populations and therefore that the moraines correspond to two closely spaced yet separate advances of similar extent. However, considering the moraine morphology and sample distribution (Fig. 5), we do not yet have strong physical evidence for this scenario.

Our dataset adds to a growing body of multiproxy evidence for late-glacial climate variability in the tropical Andes. For example, pollen records from Venezuela (Schubert and Clapperton, 1990), Colombia (Kuhry *et al.*, 1993; Van de Hammen and Hooghiemstra, 1995), Ecuador (Hansen, 1995) and Peru (Hansen, 1995) all indicate that post-LGM warming in the Tropics was interrupted by fluctuations in temperature and/or precipitation. Similarly, compelling evidence for pronounced late-glacial cold reversals is provided by the $\delta^{18}O$ ice core records from Nevados Huascarán, Peru (Thompson *et al.*, 1995), and Sajama, Bolivia (Thompson *et al.*, 1998), although the exact nature and timing of these events have yet to be established (Thompson *et al.*, 2000). Preliminary data from the new Coropuna ice core suggest that a similar reversal also is recorded at that site (Buffen, 2008).

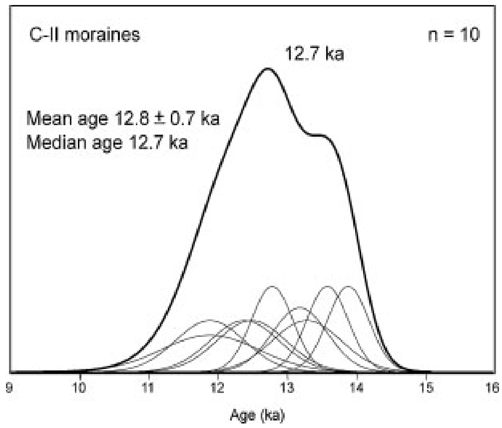

Figure 6. Probability curve of C-II ages. Mean age is given to 1σ uncertainty.

In addition to pollen and ice core records, late-glacial climate variability in the Tropics is documented by numerous moraine chronologies (Rodbell *et al.*, 2009, and references therein). Clear glacial–geomorphological evidence for post-LGM advances comes from Ecuador (e.g. Clapperton and McEwan, 1985; Clapperton *et al.*, 1997), Venezuela (Mahaney *et al.*, 2007) and Peru (e.g. Mercer and Palacios, 1977; Wright, 1984; Rodbell and Seltzer, 2000; Bromley *et al.*, 2009). With the development of surface exposure dating, our ability to resolve the timing of these events has increased greatly and glacier chronologies documenting late-glacial fluctuations now exist for several tropical Andean sites (Farber *et al.*, 2005; Smith *et al.*, 2005, 2008; Zech *et al.*, 2006, 2007; Blard *et al.*, 2009; Bromley *et al.*, 2009; Glasser *et al.*, 2009).

Collectively, these chronologies are in broad agreement. Regardless of method or scaling scheme, each record shows that the last glacial–interglacial transition was not smooth but was interrupted by glacier advances or stillstands. In this general sense, the tropical climate shares a high degree of similarity with higher latitudes, where late-glacial climate reversals are well documented. However, detailed comparison of the tropical moraine dataset reveals substantial variability among sites. For example, whereas some studies have correlated late-glacial advances with the YD (e.g. Clapperton *et al.*, 1997; Mahaney *et al.*, 2007; Glasser *et al.*, 2009), other records document advances that pre-dated the YD (Mercer and Palacios, 1977; Rodbell and Seltzer, 2000; Goodman *et al.*, 2001; Smith *et al.*, 2005; Blard *et al.*, 2009). Accepting that some of this discrepancy might be the result of methodological differences, the question remains as to what extent late-glacial climate fluctuations in the Tropics were linked to one another and to higher-latitude events.

In addressing this question, it is essential that the nature *as well as* the timing of late-glacial ice fluctuations be established. For example, when compared on the basis of age alone, the late-glacial record from Coropuna bears a striking similarity to that of Quebrada Uquian in the Cordillera Blanca (Fig. 1), site of the 'Breque' moraine (Rodbell and Seltzer, 2000). Specifically, the age range for the C-II moraines (11.9–13.9 ka) is in close agreement with the age of the Breque moraine, constrained by radiocarbon ages to 12.9–13.2 ka (Rodbell and Seltzer, 2000) and with ^{10}Be surface exposure dating to 10.4–13.2 ka (Farber *et al.*, 2005). While it is tempting to infer from this concurrence that the Breque event was regional in extent, there are important differences in moraine stratigraphy and sample distribution between Coropuna and the Cordillera Blanca site.

First, as documented by Rodbell (1991, 1993), the Breque moraine is one of four prominent landforms (termed 'Manachaque' moraines) spread over a distance of ~4.5 km and classed as late-glacial in age. In contrast, the C-II landforms on Coropuna form discrete units of single or closely paired moraines located midway between the LGM and modern ice limits. Such morphological differences between Coropuna and Quebrada Uquian reflect their different climate histories, and highlight the possibility that glaciers in the tropical Andes responded to local as well as global forcing during the late-glacial period (Rodbell *et al.*, 2009). Second, of the four Manachaque moraines, only the Breque moraine (the second youngest Manachaque limit) was dated (Rodbell and Seltzer, 2000; Farber *et al.*, 2005), whereas the C-II dataset presented here comprises ^{3}He ages from both the inner and outer moraines. Together, these considerations demonstrate that regional correlations based solely on chronological parallels, without consideration of morphology, may be inaccurate.

The late-glacial ^{3}He dataset from Coropuna spans much of the YD and ACR. In the face of present systematic uncertainties associated with surface exposure dating in tropical latitudes, however, we warn that correlation of the C-II advance with either the YD or ACR would be premature. Only minor adjustment of production rate or scaling protocol could shift the C-II chronology to be slightly younger or older than presented here. Considering the overlapping nature of the YD and ACR, this uncertainty highlights the methodological refinement needed before surface exposure dating can verify millennial- and submillennial-scale patterns in tropical glacier behaviour. Recent studies (e.g. Kelly *et al.*, 2007) increase optimism that such verification and improvement of cosmogenic nuclide production rates and international scaling models, at least at high elevations in the tropics, will be achieved soon.

Conclusions

Our C-II moraine chronology from Coropuna affords robust and directly dated evidence for an important climate event in the southern Peruvian Andes ca. 12–14 ka ago, during which glaciers occupied positions approximately half as extensive as during the LGM. The Coropuna ^{3}He dataset therefore represents an important contribution to a growing body of evidence for climate reversals during the late-glacial period in the Tropics. In addition, excellent agreement between mean and peak ages from a tightly clustered age distribution demonstrates that cosmogenic ^{3}He chronologies can be as internally consistent and precise as ^{10}Be datasets.

Acknowledgements. Funding for fieldwork was generously provided by the Dan and Betty Churchill Foundation, the Geological Society of America Graduate Student Research Grant programme, and the Sigma Xi Grants-in-aid-of-research programme. Ermitaño Zúñiga and Brian Donahue provided valuable assistance in the field. Elemental analyses were performed by Marty Yates at the University of Maine Electron Microprobe Laboratory (Department of Earth Sciences). Nat Lifton and Aaron Putnam contributed constructive input and discussion. Two reviewers and the editor provided insightful comments that greatly improved this manuscript. To all the above, our sincere thanks and gratitude. This is Lamont-Doherty Earth Observatory Contribution 7365.

Abbreviations. ACR, Antarctic Cold Reversal; LGM, Last Glacial Maximum; YD, Younger Dryas.

References

Ackert RP, Becker RA, Singer BS, *et al.* 2008. Patagonian glacier response during the late glacial–Holocene transition. *Science* **321**: 392–395.

Anderson B, Mackintosh A. 2006. Temperature change is the major driver of late-glacial and Holocene glacier fluctuations in New Zealand. *Geology* **34**: 121–124.

Balco G, Stone JO, Lifton NA, *et al.* 2008. A complete and easily accessible means of calculating surface exposure ages or erosion rates from Be-10 and Al-26 measurements. *Quaternary Geochronology* **3**: 174–195.

Blard H-P, Lavé J, Farley KA, *et al.* 2009. Late local glacial maximum in the Central Altiplano triggered by cold and locally-wet conditions during the paleolake Tauca episode (17–15 ka, Heinrich 1). *Quaternary Science Reviews* **28**: 3414–3427.

Blytt A. *Essay on the Immigration of the Norwegian Flora during Alternating Rainy and Dry Periods*. Cammermeyer: Kristiania, Norway.

Briner JP, Kaufman DS, Werner A, *et al.* 2002. Glacier readvance during the late glacial (Younger Dryas?) in the Ahklun Mountains, southwestern Alaska. *Geology* **30**: 679–682.

Bromley GRM, Schaefer JM, Winckler G, *et al.* 2009. Relative timing of last glacial maximum and late-glacial events in the central tropical Andes. *Quaternary Science Reviews* **28**: 2514–2526.

Buffen AM. 2008. *Abrupt Holocene climate change: evidence from a new suite of ice cores from Nevado Coropuna, southwestern Peru and recently exposed vegetation from the Quelccaya Ice Cap, southeastern Peru*, MS thesis Ohio State University.

Bush MB, Hansen BC, Rodbell DT, *et al.* 2005. A 17000-year history of Andean climate and vegetation change from Laguna de Chochos, Peru. *Journal of Quaternary Science* **20**: 703–714.

Clapperton CM, McEwan C. 1985. Late Quaternary moraines in the Chimborazo area, Ecuador. *Arctic and Alpine Research* **17**: 135–142.

Clapperton CM, Hall M, Mothes P, *et al.* 1997. A YD icecap in the equatorial Andes. *Quaternary Research* **47**: 13–28.

Denton GH, Hendy CH. 1994. Younger Dryas age advance of Franz Josef glacier in the Southern Alps of New Zealand. *Science* **264**: 1434–1437.

Denton GH, Alley RB, Comer GC, *et al.* 2005. The role of seasonality in abrupt climate change. *Quaternary Science Reviews* **24**: 1159–1182.

Dornbusch U. 1998. Current large-scale climatic conditions in southern Peru and their influence on snowline altitudes. *Erdkunde* **52**: 41–54.

Dornbusch U. 2002. Pleistocene and present day snowline rise in the Cordillera Ampato. *Neues Jahrbuch für Geologie und Paläontologie Abhandlungen* **225**: 103–126.

Farber DL, Hancock GS, Finkel RC, *et al.* 2005. The age and extent of tropical alpine glaciation in the Cordillera Blanca, Peru. *Journal of Quaternary Science* **20**: 759–776.

Fogwill CJ, Kubik PW. 2005. A glacial stage spanning the Antarctic Cold Reversal in Torres del Paine, Chile, based on cosmogenic exposure ages. *Geografiska Annaler* **87**: 403–408.

Glasser NF, Clemmens S, Schnabel C, *et al.* 2009. Tropical glacier fluctuations in the Cordillera Blanca, Peru between 12.5 and 7.6 ka from cosmogenic 10Be dating. *Quaternary Science Reviews* **28**: 3448–3458.

Goodman AY, Rodbell DT, Seltzer GO, *et al.* 2001. Subdivision of glacial deposits in southeastern Peru based on pedogenic development and radiometric ages. *Quaternary Research* **56**: 31–50.

Goehring BM, Kurz MD, Balco G, *et al.* 2010. A reevaluation of in situ cosmogenic ^{3}He production rates. *Quaternary Geochronology* **5**: 410–418.

Gosse JC, Evenson EB, Klein J, *et al.* 1995. Precise cosmogenic ^{10}Be measurements in western North America: support for a global YD cooling event. *Geology* **23**: 877–880.

Hansen B. 1995. A review of Lateglacial pollen records from Ecuador and Peru with reference to the Younger Dryas event. *Quaternary Science Reviews* **14**: 853–865.

Haug GH, Hughen KA, Peterson LC, *et al.* 2001. Southward migration of the Intertropical Convergence Zone through the Holocene. *Science* **293**: 1304–1308.

Herreros J, Moreno I, Taupin J-D, *et al*. 2009. Environmental records from temperate glacier ice on Nevado Coropuna saddle, southern Peru. *Advances in Geosciences* **7**: 1–8.

Hughen KA, Southon JR, Lehman SJ, *et al*. 2000. Synchronous radiocarbon and climate shifts during the last deglaciation. *Science* **290**: 1951–1954.

Kaser G. 1999. A review of the modern fluctuations of tropical glaciers. *Global and Planetary Change* **22**: 93–103.

Kelly MA, Lowell TV, Schaefer JM. 2007. A chronology of Late-Glacial and Holocene advances of Quelccaya Ice Cap, Peru, based on 10Be and radiocarbon dating. In *American Geophysical Union*, Fall Meeting 2007, abstract #PP33B-1277.

Kuhry P, Hooghiemstra H, Van Geel B, *et al*. 1993. The El Abra Stadial in the Eastern Cordillera of Colombia (South America). *Quaternary Science Reviews* **12**: 333–343.

Lal D. 1991. Cosmic ray labelling of erosion surfaces: *in situ* nuclide production rates and erosion models. *Earth and Planetary Science Letters* **104**: 424–439.

Licciardi JM, Schaefer JM, Taggart JR, *et al*. 2009. Holocene glacier fluctuations in the Peruvian Andes indicate northern climate linkages. *Science* **325**: 1677–1679.

Lifton NA, Bieber JW, Clem JM, *et al*. 2005. Addressing solar modulation and long-term uncertainties in scaling secondary cosmic rays for in situ cosmogenic nuclide applications. *Earth and Planetary Science Letters* **239**: 140–161.

Mahaney WC, Milner MW, Kalm V, *et al*. 2007. Evidence for a Younger Dryas glacial advance in the Andes of northwestern Venezuela. *Geomorphology* **96**: 199–211.

Mangerud J, Anderson ST, Berglund BE, *et al*. 1974. Quaternary stratigraphy of Norden, a proposal for terminology and classification. *Boreas* **3**: 109–128.

Mercer JH, Palacios OP. 1977. Radiocarbon dating the last glaciation in Peru. *Geology* **5**: 600–604.

Moreno PI, Kaplan MR, François JP, *et al*. 2009. Renewed glacial activity during the Antarctic cold reversal and persistence of cold conditions until 11.5 ka in southwestern Patagonia. *Geology* **37**: 375–378.

Nishiizumi K, Winterer EL, Kohl CP, *et al*. 1989. Cosmic-ray production-rates of Be-10 and Al-26 in quartz from glacially polished rocks. *Journal of Geophysical Research – Solid Earth and Planets* **94**: 17907–17915.

Oerlemans J. 2001. *Glaciers and Climate Change*. A.A. Balkema: Rotterdam.

Putnam AE, Schaefer JM, Barrell DJA, *et al*. 2010. In situ cosmogenic ^{10}Be production-rate calibration from the Southern Alps, New Zealand. *Quaternary Geochronology* **5**: 392–409.

Racoviteanu AE, Manley WF, Arnaud Y, *et al*. 2007. Evaluating digital elevation models for glaciologic applications: an example from Nevado Coropuna, Peruvian Andes. *Global and Planetary Change* **59**: 110–125.

Ramirez E, Hoffmann G, Taupin JD, *et al*. 2003. A new Andean deep ice core from Nevado Illimani (6350m), Bolivia. *Earth and Planetary Science Letters* **212**: 337–350.

Rodbell DT. 1991. *Late Quaternary glacial and climatic change in the northern Peruvian Andes*, PhD dissertation University of Colorado.

Rodbell DT. 1993. Subdivision of late Pleistocene moraines in the Cordillera Blanca, Peru, based on rock weathering features, soils and radiocarbon dates. *Quaternary Research* **39**: 133–143.

Rodbell DT, Seltzer GO. 2000. Rapid ice margin fluctuations during the Younger Dryas in the tropical Andes. *Quaternary Research* **54**: 328–338.

Rodbell DT, Smith JA, Mark BG. 2009. Glaciation in the Andes during the Lateglacial and Holocene. *Quaternary Science Reviews* **28**: 2165–2212.

Schaefer JM, Ivy-Ochs S, Wieler R, *et al*. 1999. Cosmogenic noble gas studies in the oldest landscape on earth: surface exposure ages of the Dry Valleys, Antarctica. *Earth and Planetary Science Letters* **167**: 215–226.

Schubert C, Clapperton CM. 1990. Quaternary glaciations in the northern Andes (Venezuela, Colombia, and Ecuador). *Quaternary Science Reviews* **9**: 123–135.

Schulz H, von Rad U, Erlenkeuser H. 1998. Correlations between Arabian Sea and Greenland climate oscillations of the past 10,000 years. *Nature* **393**: 54–57.

Seltzer GO, Rodbell DT, Baker PA, *et al*. 2002. Early warming of tropical South America at the last glacial-interglacial transition. *Science* **296**: 1685–1686.

Sernander R. 1908. On the evidence of post-glacial changes of climate furnished by the peat mosses of northern Europe. *Geologiska Föreningens i Stokholm Förhaldlinger* **30**: 365–478.

Smith CA, Lowell TV, Caffee MCW. 2008. Lateglacial and Holocene cosmogenic surface exposure age glacial chronology and geomorphological evidence for the presence of cold-based glaciers at Nevado Sajama, Bolivia. *Journal of Quaternary Science* **24**: 360–372.

Smith JA, Seltzer GO, Rodbell DT, *et al*. 2005. Early local last glacial maximum in the tropical Andes. *Science* **308**: 678–681.

Smith JA, Mark BG, Rodbell DT. 2008. The timing and magnitude of mountain glaciation in the tropical Andes. *Journal of Quaternary Science* **23**: 609–634.

Solomina O, Jomelli V, Kaser G, *et al*. 2007. Lichenometry in the Cordillera Blanca, Peru: 'Little Ice Age' moraine chronology. *Global and Planetary Change* **59**: 225–235.

Stone JO. 2000. Air pressure and cosmogenic isotope production. *Journal of Geophysical Research* **105**: 23753–23759.

Thompson LG, Mosley-Thompson E, Davis ME, *et al*. 1995. Late Glacial Stage and Holocene ice core records from Huascarán, Peru. *Science* **269**: 46–50.

Thompson LG, Davis ME, Mosley-Thompson E, *et al*. 1998. A 25,000-year tropical climate history from Bolivian ice cores. *Science* **282**: 1858–1864.

Thompson LG, Mosley-Thompson E, Henderson KA. 2000. Ice-core palaeoclimate records in tropical South America since the Last Glacial Maximum. *Journal of Quaternary Science* **15**: 377–394.

Van der Hammen T, Hooghiemstra H. 1995. The El Abra stadial, a Younger Dryas equivalent in Colombia. *Quaternary Science Reviews* **14**: 841–851.

Venturelli G, Fragipane M, Weibel M, *et al*. 1978. Trace element distribution in the Cainozoic lavas of Nevado Coropuna and Andagua Valley, Central Andes of southern Peru. *Bulletin of Volcanology* **41**: 213–228.

Wang YJ, Cheng H, Edwards RL, *et al*. 2001. A high-resolution absolute-dated Late Pleistocene monsoon record from Hulu Cave, China. *Science* **294**: 2345–2348.

Weibel M, Frangipane-Gysel M, Hunziker JC. 1978. Ein Beitrag zur Vulkanologie Süd-Perus. *Geologische Rundschau* **67**: 243–252.

Winckler G, Anderson RF, Schlosser P. 2005. Equatorial Pacific productivity and dust flux during the Mid-Pleistocene climate transition. *Paleoceanography* **20**: PA4025.

Wright HE. 1984. Late glacial and late Holocene moraines in the Cerros Cuchpanga, central Peru. *Quaternary Research* **21**: 275–285.

Zech R, Kull C, Veit H. 2006. Late Quaternary glacial history in the Encierro Valley, northern Chile (29°S), deduced from ^{10}Be surface exposure dating. *Palaeogeography, Palaeoclimatology, Palaeoecology* **234**: 277–286.

Zech R, Kull C, Kubik PW, *et al*. 2007. LGM and Late Glacial glacier advances in the Cordillera Real and Cochabamba (Bolivia) deduced from ^{10}Be surface exposure dating. *Climate of the Past* **3**: 623–635.

Zech R, May J-H, Kull C, *et al*. 2008. Timing of the late Quaternary glaciation in the Andes from $\sim$15 to 40°S. *Journal of Quaternary Science* **23**: 635–647.